Acta Crystallographica Section D
Biological Crystallography
ISSN 0907-4449

Structural basis for discrimination between oxyanion substrates or inhibitors in aspartate-β-semialdehyde dehydrogenase

Christopher R. Faehnle, Julio Blanco and Ronald E. Viola*

Department of Chemistry, University of Toledo, Ohio 43606, USA

Correspondence e-mail: ron.viola@utoledo.edu

Received 26 August 2004
Accepted 18 October 2004

PDB References: ASADH–arsenate, 1ta4, r1ta4sf; ASADH–periodate, 1tb4, r1tb4sf.

The reversible dephosphorylation of β-aspartyl phosphate to L-aspartate-β-semialdehyde (ASA) in the aspartate biosynthetic pathway is catalyzed by aspartate-β-semialdehyde dehydrogenase (ASADH). The phosphate that is present to activate the aspartate carboxyl group is held in a separate and distinct binding site once removed and prior to its release from the enzyme. This site had been shown to be selective for tetrahedral oxyanions, with several competitive inhibitors and alternative substrates previously identified for the reverse reaction. Structural studies have now shown that the most potent oxyanion inhibitor (periodate) and a good alternative substrate (arsenate) each occupy the same catalytic phosphate-binding site. However, a rotation of a threonine side chain (Thr137) in the periodate complex disrupts an important hydrogen-bonding interaction with an active-site glutamate (Glu243) that participates in substrate orientation. This subtle change appears to be the difference between a substrate and an inhibitor of this enzyme.

1. Introduction

L-Aspartate-β-semialdehyde (ASA) occupies the first branch point in the pathway that ultimately leads to the synthesis of lysine, methionine, threonine and isoleucine (Cohen, 1983; Viola, 2001). The commitment step in this amino-acid biosynthetic pathway requires the activation of aspartate through a phosphorylation catalyzed by aspartokinase. The resulting β-aspartyl phosphate (βAP) is then reductively dephosphorylated to ASA by the enzyme aspartate-β-semialdehyde dehydrogenase (ASADH). While phosphate is the physiological oxyanion used for the activation of aspartate, other oxyanions have been shown to bind at the phosphate catalytic site in ASADH. Tellurate, phosphonate and tungstate are each moderate competitive inhibitors *versus* phosphate, while periodate is the most potent oxyanion inhibitor, with a K_i of 0.2 m*M* (Kish & Viola, 1999). This site will also accept vanadate and arsenate as alternative substrates in the reverse reaction catalyzed by ASADH (Fig. 1), with k_{cat} values comparable to that for phosphate and a K_m for vanadate that is 20-fold lower than that for phosphate (Kish & Viola, 1999). Cacodylate (dimethylarsenate), a common buffer used in crystallization trials, has also recently been found to be a weak alternative substrate for ASADH (Blanco, Moore, Faehnle & Viola, 2004).

Several bacterial ASADHs have been purified and structurally characterized as the apoenzyme (Hadfield *et al.*, 1999), various substrate complexes (Blanco, Moore, Kalabeeswaran *et al.*, 2003; Blanco, Moore & Viola, 2003; Hadfield *et al.*, 1999, 2001) and an intermediate complex (Blanco, Moore & Viola, 2003). The function of the cysteine–histidine catalytic dyad of

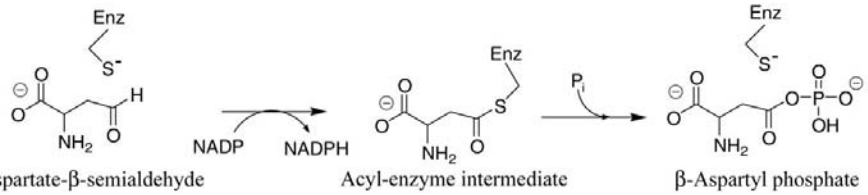

Figure 1
An abbreviated mechanism of the reaction catalyzed by aspartate β-semialdehyde dehydrogenase in the reverse (non-physiological) direction.

Table 1
Data-collection statistics for the ASADH–oxyanion complexes.

Values in parentheses are for the highest resolution shell.

	Arsenate complex	Periodate complex
Wavelength (Å)	1.54	1.54
Space group	$P2_12_12$	$P2_12_12$
Unit-cell parameters		
a (Å)	113.8	114.0
b (Å)	54.8	55.1
c (Å)	57.5	57.6
Resolution (Å)	2.28	2.15
No. measured observations	75897	144074
No. unique observations	18047	20457
Completeness (%)	95.2 (97.8)	99.9 (100)
R_{sym} (%)	6.7 (32.2)	6.3 (35.9)
Average $\langle I/\sigma(I)\rangle$	20.5 (3.9)	30.4 (6.3)

Table 2
Structural refinement statistics for the ASADH complexes.

Values in parentheses are for the highest resolution shell.

	Arsenate complex	Periodate complex
Refinement		
Resolution range (Å)	50–2.30	50–2.30
R_{cryst} (%)	20.0 (32.0)	20.0 (29.0)
R_{free} (%)	27.5 (40.0)	27.4 (34.0)
No. of protein atoms	2755	2755
No. non-protein atoms	10	5
No. water molecules	255	311
Stereochemistry		
R.m.s.d. for bond lengths (Å)	0.011	0.008
R.m.s.d. for bond angles (°)	1.24	1.08
Residues in the Ramachandran plot		
Most favored region (%)	89.0	92.5
Additional allowed regions (%)	10.4	6.8
Generously allowed regions (%)	0.6	0.7

ASADH from *Haemophilus influenzae* (Blanco, Moore, Faehnle & Viola, 2004) and the roles of several ASA and phosphate-binding groups in this enzyme have also been determined (Blanco, Moore, Faehnle, Coe *et al.*, 2004). Here, we examine the binding of two phosphate analogs, a potent competitive inhibitor (periodate) and an efficient alternative substrate (arsenate), to assess the structural determinants that can distinguish between oxyanion inhibitor binding and oxyanion substrate binding.

2. Experimental procedures

2.1. Preparation, purification and crystallization of ASADH

The *asd* gene from *H. influenzae* that encodes ASADH was subcloned into a pET expression system (pET41a/*asd*) and overexpressed as described previously (Moore *et al.*, 2002). The enzyme was purified to homogeneity using our previously published protocol (Moore *et al.*, 2002).

H. influenzae ASADH was concentrated by ultrafiltration (Millipore) to >10 mg ml^{-1} and dialyzed against 10 m*M* sodium HEPES pH 7.0 containing 1 m*M* EDTA and 1 m*M* DTT. Crystallization conditions were obtained by hanging-drop vapor diffusion by optimizing initial conditions identified using the PEG/Ion Screen (Hampton Research). Crystals of ASADH were grown at 293 K in 1:1 mixtures of enzyme and precipitant solution and diffraction-quality crystals were obtained with 22–24% PEG 4000 as the precipitant in the presence of 0.2 *M* ammonium acetate and Tris buffer pH 8.5.

2.2. Formation of the enzyme–oxyanion complexes

The apoenzyme crystals obtained under these conditions were complexed by soaking with each of the oxyanions for 1 h prior to harvesting. A harvesting solution was prepared (26% PEG 3350, 0.2 *M* ammonium acetate, 100 m*M* arsenate or periodate, 0.1 *M* Tris–HCl pH 8.5 containing 20% glycerol) and this solution was introduced stepwise over a period of approximately 1 h in order to minimize damage to the crystals, which were subsequently flash-frozen for X-ray diffraction data collection.

2.3. Data collection and processing

Diffraction data from crystals of the ASADH complexes with arsenate and periodate were collected on a rotating-anode diffractometer equipped with an R-AXIS IV detector (detector distance 160 mm; 1° oscillation per image). The images from each data set were processed and scaled using *CrystalClear* (Rigaku/MSC). Data-collection statistics for each of these data sets are summarized in Table 1.

2.4. Structure solution and refinement

Data sets of the ASADH oxyanion complexes belong to space group $P2_12_12$ and give a single subunit in the asymmetric unit. These structures were solved by molecular replacement using a subunit of the *H. influenzae* apo-ASADH dimer (PDB code 1nwc) as the search model. The rotation and translation searches were carried out by the program *MOLREP* (Vagin & Teplyakov, 1997) as implemented in the *CCP*4 suite of programs (Collaborative Computational Project, Number 4, 1994). The initial model was subjected to rigid-body refinement followed by restrained refinement with *REFMAC*5 (Murshudov *et al.*, 1997). Manual corrections to the model were made with *XtalView* (McRee, 1999). The quality of the final model was confirmed with *PROCHECK* (Laskowski *et al.*, 1993) and is quite good despite the relatively high R values for data at this resolution. The refined coordinates have each been deposited with the PDB; the final refinement statistics are listed in Table 2.

3. Results and discussion

The ASADHs from a variety of organisms encompass a considerable diversity of sequence homologies, ranging from as little as 10% to as high as 95% sequence identity to the *Escherichia coli* enzyme. Despite this sequence diversity, the identity of the core active-site functional groups and the essential catalytic function of this enzyme have been preserved throughout evolution. Here, we examine structures of *H. influenzae* ASADH complexes with oxyanion analogs of the substrate phosphate, with the aim of identifying key structural changes that can distinguish between a substrate and an inhibitor.

3.1. Structure of the arsenate complex of ASADH

Diffraction data were collected at our home X-ray source from crystals of *H. influenzae* ASADH with arsenate diffused into the phosphate-binding site. Arsenate has been shown to be an alternative substrate (Kish & Viola, 1999) with kinetic parameters comparable to those of phosphate for the reverse reaction (Fig. 1). Crystals of this complex diffracted to 2.3 Å and were indexed and refined in space group $P2_12_12$. The overall structure of the arsenate–ASADH complex (PDB code 1ta4) is virtually identical to the previously determined structure of *H. influenzae* ASADH with bound phosphate (Blanco, Moore & Viola, 2003). In this newly determined structure, two molecules of arsenate are bound per enzyme subunit (Fig. 2*a*): one in the catalytic oxyanion site and the second in an ancillary phosphate-binding site that was detected in the ASA–phosphate catalytic intermediate enzyme structure (Blanco, Moore & Viola, 2003). As was seen with the previously determined phosphate-bound structure, the electron density of arsenate in this ancillary site is weaker than the density in the catalytic oxyanion site. This observation is consistent with either a lower occupancy or a higher oxyanion mobility at this secondary binding site. The *B* factor calculated for the arsenate bound in the catalytic site is 56 Å^2, while the arsenate in the ancillary binding site has a *B* factor of 75 Å^2. This higher thermal mobility is consistent with the weaker density observed at this ancillary site.

3.2. Structure of the periodate complex of ASADH

Periodate has been found to be the best oxyanion inhibitor of ASADH (Kish & Viola, 1999). Crystals of the periodate–enzyme complex diffracted to 2.2 Å and were indexed in the same space group as the arsenate structure. Again, the overall structure of this periodate–enzyme complex (PDB code 1tb4) is essentially unchanged from the previous oxyanion structures that have been determined. The inhibitor periodate is also found to occupy the same position (within 0.3 Å) in the oxyanion catalytic binding site as the oxyanion substrates that have been studied (Fig. 2*b*). However, unlike the binding of phosphate or arsenate, only a single molecule of periodate is bound per subunit of ASADH. Periodate does not appear to bind at the ancillary site that is adjacent to the active site.

3.3. A comparison of oxyanion-binding sites

The position of the bound arsenates and the identity of the protein ligands to the arsenates are identical to those previously seen in the phosphate-bound structure (Fig. 3*a*). The arsenate in the catalytic site is coordinated in a tetrahedral fashion by the side-chain functional groups of Arg103, Lys246 and Asn135 and by a water molecule, with each serving as a direct ligand (Fig. 3*b*). In the inhibitor structure the periodate bound at the catalytic site also utilizes this same ligand set (Fig. 3*c*). There are no unusually short donor-atom distances to periodate and nothing in the geometry at this site distinguishes the coordination of this inhibitor from the interactions between the enzyme and its oxyanion substrates. Thus, this comparison between the structures of a substrate and an inhibitor bound at the catalytic oxyanion site does not resolve the question of how the enzyme can make a functional distinction.

The arsenate at the ancillary site is coordinated through interactions with Lys246 (as a shared ligand with arsenate at the catalytic site), Lys242, Ser100 and a water molecule (Fig. 3*b*). Each of these ligands is the same as the ligands to phosphate at this site, although the side chain of Lys242 does appear to adopt a different conformation in the arsenate complex while still maintaining the same oxyanion coordination role.

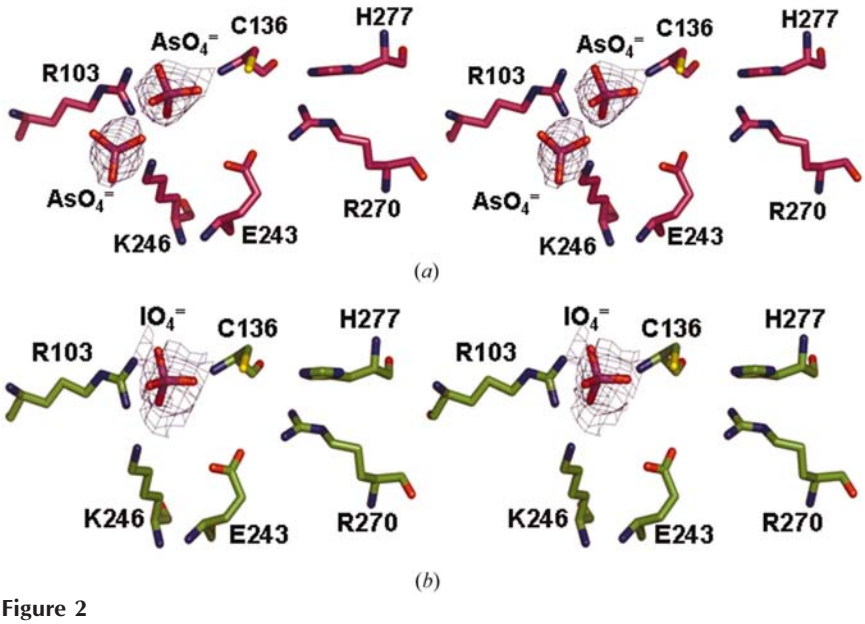

Figure 2
Stereoview of the $F_o - F_c$ electron density for oxyanions bound to *H. influenzae* ASADH. (*a*) Arsenate bound in the catalytic site adjacent to Cys136 and a second molecule of arsenate bound in the ancillary site. (*b*) Periodate bound only in the catalytic site.

Table 3
Switch of hydrogen-bonding partners for Thr137.

Enzyme form	Distance to Asn135† (Å)	Distance to Glu243† (Å)
Apoenzyme	<2.7‡	3.58
ASA–phosphate complex	3.40	2.88
Arsenate complex	3.40	2.99
Periodate complex	2.72	3.59
E243D mutant	2.79	4.12

† Distances between the hydroxyl O-atom donor on Thr137 and the carbonyl or carboxyl O-atom acceptor. ‡ The nearly continuous density between the donor and acceptor at this resolution precludes an accurate measurement of this distance.

3.4. The differences between substrate and inhibitor binding to ASADH

A well established mode of substrate or substrate-analog inhibition is the presence of a second binding site, the occupation of which will result in enzyme inhibition. In the case of ASADH, an ancillary oxyanion site has been identified that binds phosphate and now has also been shown to bind arsenate. However, both of these oxyanions are substrates for ASADH and show no evidence of either substrate inhibition or non-Michaelis–Menten kinetics, even at very high concentrations. In contrast, periodate is a fairly potent inhibitor of ASADH, yet does not appear to bind at this ancillary site. This raises the critical question of why periodate is an inhibitor of ASADH while the other oxyanions are substrates.

Charge-distribution calculations on a series of oxyanions found to interact with ASADH showed that those anions that are either alternative substrates or inhibitors have the highest negative-charge density on the peripheral O atoms (Kish & Viola, 1999). The only anomaly in this analysis is periodate, which is the best inhibitor but has significantly lower charge density on O atoms than some of the non-inhibitory oxyanions. While this first periodate-bound structure shows nearly identical binding interactions at the catalytic oxyanion site, there are some subtle shifts in several amino-acid side chains that appear to be responsible for its inhibitory character. In the apoenzyme the side-chain hydroxyl group of Thr137 forms a hydrogen bond with Asn135 and this pairing prevents any interactions with the active-site Glu243 (Table 3). Upon binding of either oxyanion substrate, phosphate or arsenate, Thr137 switches hydrogen-bonding partners through a 60° rotation that disrupts the interaction with Asn135 (Fig. 4). This new conformation moves the threonine hydroxyl group by 1.4 Å, into position to now interact with and help to orient Glu243, an important substrate-binding group. Glu243 remains in this substrate-binding position in the arsenate structure and this hydrogen bond with the Thr137 hydroxyl group persists, even in the absence of bound ASA. Thus, it appears that the presence of an oxyanion substrate in the active site helps to position this group to interact with ASA. However, in the periodate structure this threonine does not change position and switch partners. In this newly determined inhibitor-bound structure, Thr137 remains hydrogen-bonded to Asn135, the amino acid adjacent to the active-site cysteine nucleophile, causing a shift of this side chain by 0.4 Å relative to its position in the phosphate and arsenate structures. Since Thr137 is now oriented away from Glu243, it cannot stabilize

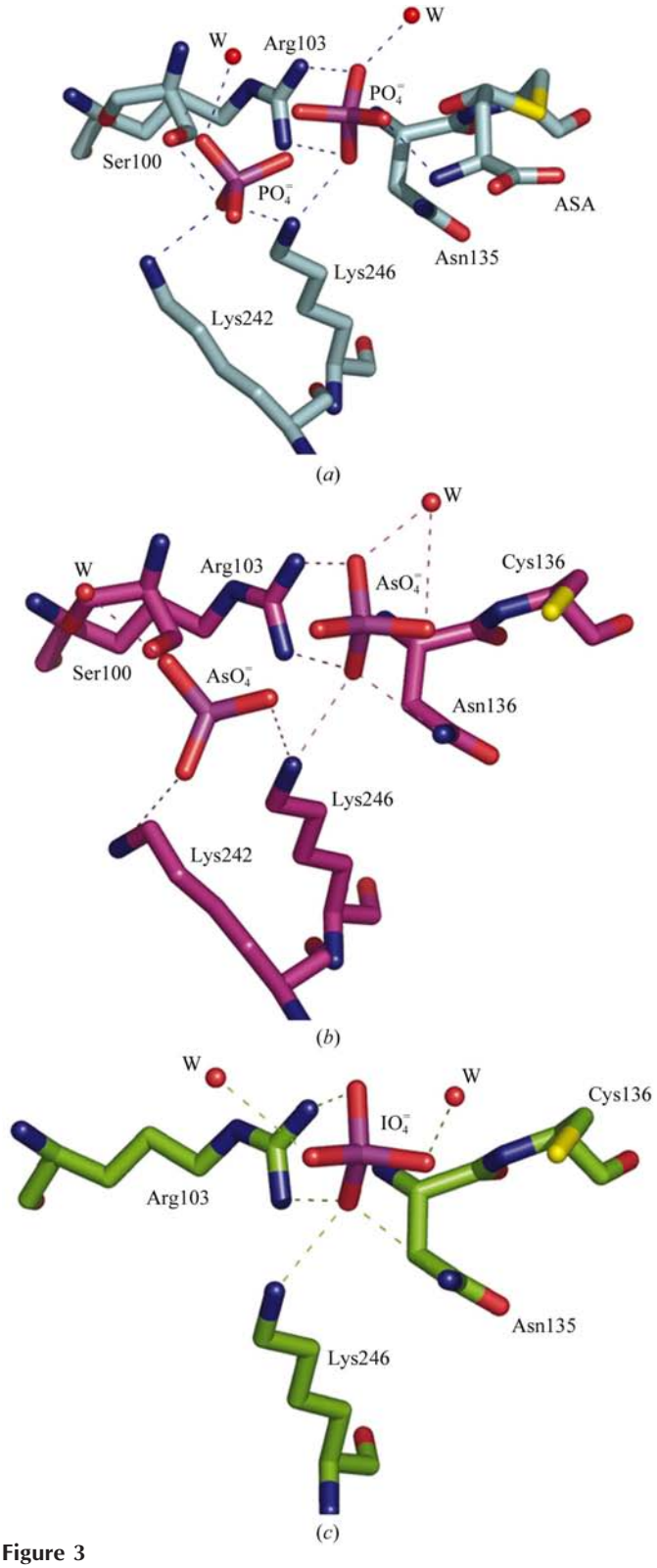

Figure 3
Comparison of the oxyanion-binding sites. Each of the oxyanions utilizes the same ligands in the catalytic and ancillary binding sites. (*a*) Binding of the substrate phosphate at both sites. (*b*) Binding of the alternative substrate arsenate at both sites. (*c*) Binding of the inhibitor periodate at only the catalytic site.

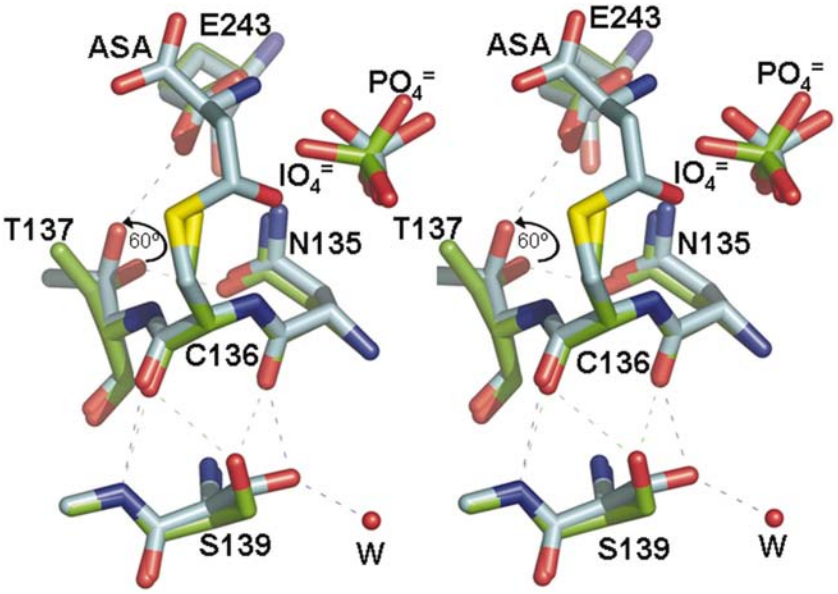

Figure 4
Stereoview of an overlay of *H. influenzae* ASA–phosphate structure (blue) and the periodate-bound structure (green). Periodate binding at only the catalytic site results in a reorientation of Thr137 that disrupts the hydrogen bond to an important substrate-orienting group (Glu243). Ser139 is repositioned in the periodate structure and forms a new hydrogen-bonding interaction with the backbone carbonyl of the active-site nucleophile (Cys136).

the position of this side chain (Fig. 4). The distances between Thr137 and its potential hydrogen-bonding partners are dramatically different in the periodate complex compared with either the phosphate or arsenate complexes, and are in fact closer to the distances observed for the apoenzyme (Table 3).

The role of Glu243 in orienting the bound ASA substrate had been ascertained by mutating this residue to the structurally related amino acid aspartate. The catalytic activity of this E243D mutant is about 1% of the native enzyme (Blanco, Moore, Faehnle, Coe *et al.*, 2004) despite only a subtle shift in the position of the bound ASA. There is also no significant repositioning of the catalytic and substrate-binding functional groups, so it was not clear what has caused this loss of activity. The Thr137 hydroxyl group in this mutant structure is now seen to be oriented in a similar position to that in the periodate complex, making the same hydrogen-bonding contact that is observed in this inhibitor structure and in the apoenzyme (Table 3). Thus, the rotation of this functional group may also be the explanation for the dramatic loss of activity observed for this conservative mutation.

In addition to the movements described above, an active-site serine (Ser139) in the periodate structure has rotated into position to form a hydrogen bond with the backbone carbonyl of Cys136, the active-site nucleophile in ASADH. This interaction is not observed in either the phosphate or the arsenate structures and could lead to inhibition by altering the position of this essential cysteine catalytic group. An overlay of the periodate structure with the ASA–phosphate structure shows this reorientation of Ser139 and a corresponding shift in the position of the Cys136 thiolate group by about 0.6 Å (Fig. 4). However, when this periodate structure is compared with the arsenate structure that also has a reoriented Ser139, no corresponding shift is seen for the Cys136 side chain. It appears that the shift in the position of the Cys136 thiolate is caused primarily by the binding of ASA in the phosphate structure and not by the binding of an oxyanion inhibitor in the phosphate site.

4. Conclusions

The phosphate-binding site of ASADH can accommodate several tetrahedral oxyanion analogs leading to different functional consequences. Oxyanion substrates and inhibitors bind at the same position and utilize the same set of binding ligands. However, the binding of the inhibitor periodate triggers a rotation of a threonine hydroxyl group that prevents it from stabilizing the position of an important substrate-orienting group. Thus, only subtle shifts in side chains that are not directly involved in substrate binding or catalysis can lead to a sequence of events with adverse consequences for a fine-tuned enzyme catalyst.

This work was supported by a grant from the National Science Foundation (MCB0196107). The authors thank the *E. coli* Genetic Stock Center (Yale University) for providing the *asd*-deficient cell line.

References

Blanco, J., Moore, R. A., Faehnle, C. R., Coe, D. M. & Viola, R. E. (2004). *Acta Cryst.* D**60**, 1388–1395.
Blanco, J., Moore, R. A., Faehnle, C. R. & Viola, R. E. (2004). *Acta Cryst.* D**60**, 1808–1815.
Blanco, J., Moore, R. A., Kalabeeswaran, V. & Viola, R. E. (2003). *Protein Sci.* **12**, 27–33.
Blanco, J., Moore, R. A. & Viola, R. E. (2003). *Proc. Natl Acad. Sci. USA*, **100**, 12613–12617.
Cohen, G. N. (1983). *Amino Acids: Biosynthesis and Genetic Regulation*, edited by K. M. Herrmann & R. L. Somerville, pp. 147–171. Reading, MA, USA: Addison–Wesley.
Collaborative Computational Project, Number 4 (1994). *Acta Cryst.* D**50**, 760–763.
Hadfield, A. T., Kryger, G., Ouyang, J., Petsko, G. A., Ringe, D. & Viola, R. E. (1999). *J. Mol. Biol.* **289**, 991–1002.
Hadfield, A. T., Shammas, C., Kryger, G., Ringe, D., Petsko, G. A., Ouyang, J. & Viola, R. E. (2001). *Biochemistry*, **40**, 14475–14483.
Kish, M. M. & Viola, R. E. (1999). *Inorg. Chem.* **38**, 818–820.
Laskowski, R. A., MacArthur, M. W., Moss, D. S. & Thornton, J. M. (1993). *J. Appl. Cryst.* **26**, 283–291.
McRee, D. E. (1999). *J. Struct. Biol.* **125**, 156–165.
Moore, R. A., Bocik, W. E. & Viola, R. E. (2002). *Protein Expr. Purif.* **25**, 189–194.
Murshudov, G. N., Vagin, A. A. & Dodson, E. J. (1997). *Acta Cryst.* D**53**, 240–255.
Vagin, A. A. & Teplyakov, A. (1997). *J. Appl. Cryst.* **30**, 1022.
Viola, R. E. (2001). *Acc. Chem. Res.* **34**, 339–349.